Ab initio study of magnetic and structural properties of Fe-Ga alloys

Mariya Matyunina[1,*], *Mikhail* Zagrebin [1,2], *Vladimir* Sokolovskiy [1,3] and *Vasiliy* Buchelnikov[1]
[1] Chelyabinsk State University, 454 001 Chelyabinsk, Russia
[2] National Research South Ural State University, 454001 Chelyabinsk, Russia
[3] National University of Science and Technology 'MIS&S', 119991 Moscow, Russia

Abstract. The structural and magnetic properties for a series of $Fe_{100-x}Ga_x$ alloys (x = 18 – 30 at.%) are studied in the framework of first-principles calculations and Monte Carlo simulations. The both, general gradient approximation and local density approximation are considered for the exchange-correlation functional. The ground state *ab initio* calculations are performed for both $D0_3$ and $L1_2$ crystal structures. It is shown that for general gradient approximation, the optimized lattice parameters and total magnetic moments are found in the better agreement with experimental ones. Using the calculated exchange coupling constants for studied compositions, Curie temperatures are estimated by means of Monte Carlo simulations of Heisenberg Hamiltonian.

1 Introduction

The Fe-Ga alloys are successful magnetostrictive materials which are very attractive to use in magnetostrictive actuators, sensor and spintronic devices [1-8]. Doping Ga up to 30 at% into the bcc Fe enhances greatly both the value of tetragonal magnetostriction λ_{001} in the [001] direction and ductility [1-3]. Experimental investigations of $Fe_{100-x}Ga_x$ alloys have shown that the value of tetragonal magnetostriction λ_{001} has two peaks (395×10^{-6} and 350×10^{-6}) for composition with 19 and 27 at% Ga concentration at room temperature, respectively [2].

In the past decade, Fe-Ga alloys became the objects of intensive experimental and theoretical studies. For instance, the experimental investigations of magnetic and structural properties by means of X-ray diffraction, mechanical spectroscopy techniques, dynamical mechanical analyzer, neutron diffraction, Mössbauer spectroscopy can be found in Refs. [2-8]. The theoretical studies of Fe-Ga and related alloys using first principles approach are presented in Refs. [9-16]. Wang et al. [12-13] and Zhang et al. [14-16] calculated the magnetostrictive coefficient λ_{001}, strain-dependent total energies and magnetocrystalline anisotropy (MAE) of the $Fe_{100-x}Ga_x$ ($5 < x \leq 25$). The results were found in a good agreement with experimental data. Wu [9] considered an enhancement in magnetostriction for ordered $D0_3$, $L1_2$, and B2-like structures in $Fe_{75}Ga_{25}$ due to a splitting of Fe 3*d*-bands in minority spin channel around Fermi level. Khmelevska et al. [10] proposed the more complex origin of giant magnetostriction in $Fe_{100-x}Ga_x$ ($0 < x < 25$) due to disorder effects in the framework of coherent potential approximation (CPA).

The aim of this paper is a complex study of magnetic and structural properties of $Fe_{100-x}Ga_x$ (x = 18 – 30 at%) alloys by the density of functional theory with the different approximations for the exchange-correlation energy and finite-temperature Monte Carlo (MC) simulations.

2 Computation details

In the first step of our calculations, we have done the geometric optimization of crystal structures by using the SPR-KKR (spin polarized relativistic Korringa-Kohn-Rostoker) software package based on the Korringa-Kohn-Rostoker Green's function [17]. For all *ab initio* calculations, the exchange-correlation energy was treated by the generalized gradient approximation in the Perdew-Burke-Ernzerhof (GGA-PBE) formulation [18] and the local density approximation in the form of Vosko-Wilk-Nusair (LDA-VWN) [19]. For self-consistent cycles (SCF) calculations, 6348 ***k*** points were generated by a ***k***-mesh grid of 45^3. The total energy for all calculations converged to 0.01 mRy. To construct off-stoichiometric compositions, the CPA was considered.

To perform the crystal structure optimization, we used two face-centered cubic $L1_2$ ($Pm\bar{3}m$, #221) and body-centered cubic $D0_3$ ($Fm\bar{3}m$, #225) structures with their associated unit cells, which contain 4 atoms. Note that the stoichiometric $Fe_{75}Ga_{25}$ (Fe_3Ga) can crystallize in the $D0_3$ structure [6]. There are three Fe atoms per unit cell belonging to two different sublattices. For the formation of non-stoichiometric compositions of $Fe_{100-x}Ga_x$, Ga atoms taken in the required percentage were fixed at next sites as listed in Table 1.

In the second step, using the optimized lattice parameters obtained within GGA-PBE and LDA-WVN

* Corresponding author: matunins.fam@mail.ru (M. Matyunina)

approximations, the calculations of exchange interaction parameters J_{ij} for both structures were performed. The Heisenberg exchange coupling constants were calculated using the expression proposed by Liechtenstein et al. [20]. All calculations converged to 0.01 mRy of total energy.

Table 1. The atomic distribution for off-stoichiometric $Fe_{100-x}Ga_x$ alloys with the $L1_2$ and $D0_3$ structures

Space group	Wyckoff positions	x<25%	x=25%	x>25%
		Atoms	Atoms	Atoms
$Pm\bar{3}m$ (#221)	1*a*: 0, 0, 0	Ga, Fe	Ga	Ga
	3*c*: 0, 0.5, 0.5	Fe	Fe	Ga, Fe
$Fm\bar{3}m$ (#225)	4*a*: 0, 0, 0	Ga, Fe	Ga	Ga
	4*b*: 0.5, 0.5, 0.5	Fe	Fe	Ga, Fe
	8*c*: 0.25, 0.25, 0.25	Fe	Fe	Fe

The final step is the Curie temperature estimation with the help of the MC simulations of the three-dimensional Heisenberg model ($H_{mag} = -\sum_{\langle ij \rangle} J_{ij}\mathbf{S}_i\mathbf{S}_j$). Here $\mathbf{S}_i = (S_i^x, S_i^y, S_i^z)$ is a classical magnetic degree of freedom $|\mathbf{S}_i| = 1$. The exchange parameters J_{ij} and partial magnetic moments μ were taken as input parameters from *ab initio* calculations. The model lattice with periodic boundary conditions for $Fe_{75}Ga_{25}$ alloy contains 2826 (3300) Fe and 1099 (1331) Ga atoms for $D0_3$ ($L1_2$) phase, respectively. The MC simulations were carried out using the Metropolis algorithm [21]. As time unit, we used on MC step consisting of N attempts to change the spin variables. The total number of MC steps per the temperature step was 10^6. The magnetic order parameter m and total magnetization M are defined by the following way

$$m^{Fe} = \frac{1}{N^{Fe}} \sum_i \sqrt{(S_i^{Fe,x})^2 + (S_i^{Fe,y})^2 + (S_i^{Fe,z})^2}\,, M = 3\mu_{Fe} m^{Fe},$$

here μ_{Fe} is the magnetic moment of Fe taken from first principals calculations.

To estimate the Curie temperature from $M(T)$ curves, we plotted the $M^{1/\beta}(T)$ function that decreases almost linearly with increasing temperature. The Curie temperature can be evaluated at the intersection of a $M^{1/\beta}$ curve with the T axis. Here, β is the critical index and it is equal to 0.3646 for the three-dimensional Heisenberg model.

3 Results and discussions

3.1. Lattice parameters and magnetic moments

In this subsection, we present the results of calculations of the optimized lattice parameters and total magnetic moments for studied compositions with $D0_3$ and $L1_2$ structures.

Fig. 1 shows the variation of equilibrium lattice parameter a_0 (which corresponds to a minimum value of energy E_0) as a function of Ga concentration for both $D0_3$ and $L1_2$ structures of $Fe_{100-x}Ga_x$ alloys in comparison with available experimental data taken from Ref. [22]. Here we present results obtained by using GGA-PBE and LDA-WVN approximations for the exchange-correlation functional.

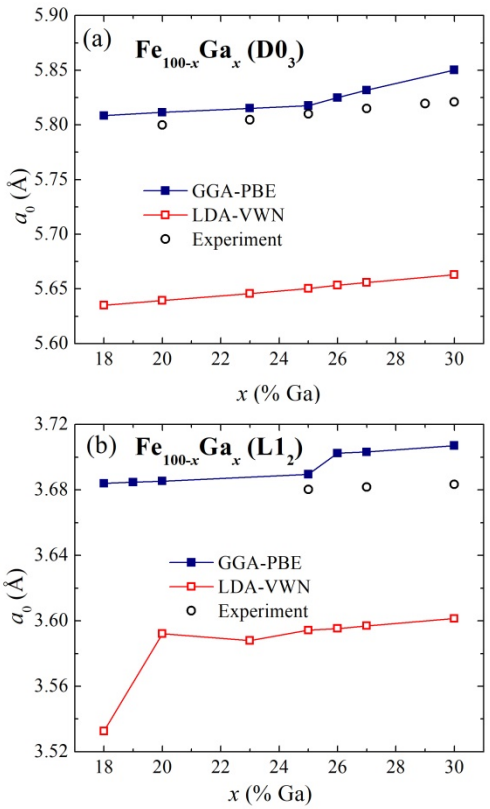

Fig. 1. The calculated equilibrium lattice parameter (a_0) as a function of Ga concentration (x) for the (a) $D0_3$ and (b) $L1_2$ structures of $Fe_{100-x}Ga_x$ alloys in comparison with experimental data. The experimental data were taken from [22].

Our calculation have shown that for both $D0_3$ and $L1_2$ structures, lattice constant increases with increasing Ga concentration. For both bcc and fcc structures, the results obtained within the GGA-PBE approximation are in the better agreement with the experimental data than those obtained for the LDA-VWN approximation.

In Fig. 2, we present the calculated total magnetic moments for the studied compositions $Fe_{100-x}Ga_x$ (x = 18 – 30 at%) with $D0_3$ and $L1_2$ structures. It is clearly seen that for both structures, the total magnetic moment decreases with increasing Ga content. Concerning the effect of choice for the exchange-correlation potential, we can see the similar trend as in Fig. 1. Namely, for both $D0_3$ and $L1_2$ structures, the values of magnetization obtained within the GGA-PBE approximation are closer to the experimental data taken from [8].

Generally, according to Ref. [23], exchange-correlation functional GGA reproduces the equilibrium volume of 3d-metals better than the LDA. Believe that the LDA fails to correctly reproduce the ground state bcc structure of Fe because the magnetic contribution to the stabilization of the bcc structure is weakened by this exchange-correlation functional while at the same time

the GGA corrects the volume and thereby the magnetic contribution. We could equally well say that for the ground state calculations of Fe-Ga alloys with different phases the method of Green's function within GGA-PBE gives better results than LDA-VWN.

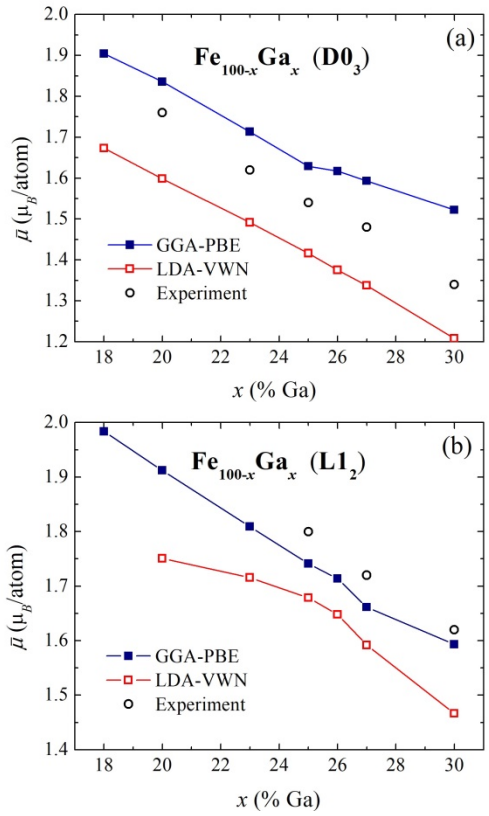

Fig. 2. The calculated total magnetic moment $\bar{\mu}$ per atom (in μ_B/ atom) as a function of Ga concentration (x) for the (a) (a) $D0_3$ and (b) $L1_2$ crystal structures of $Fe_{100-x}Ga_x$ alloys in comparison with experimental data. The experimental data were taken from [8].

3.2. Magnetic exchange interaction and Curie temperature

The knowledge of optimized lattice parameters allows us to calculate further the Heisenberg exchange interaction parameters J_{ij} for both bcc and fcc structures of $Fe_{100-x}Ga_x$ alloys. Since the results of lattice parameter calculations obtained within the LDA-VWN differ significantly from the experimental ones, we further used only the set of a_0 calculated within the GGA-PBE. Nevertheless, the calculations of J_{ij} parameters were calculated using both approaches: GGA-PBE and LDA-WVN. As a result, we will use two new denotations: GGA-GGA and GGA-LDA. The first (second) one denotes the J_{ij} calculations within the GGA-PBE (LDA-WVN) using the set of a_0 calculated within the GGA-PBE, respectively.

Fig. 3 displays the magnetic exchange parameters for $D0_3$ and $L1_2$ phases of the $Fe_{73}Ga_{27}$ alloy as a function of the distance between atoms. The $Fe_{73}Ga_{27}$ composition is of interest due to the presence of structural phase transition between $D0_3$ and $L1_2$ phases [4]. For both phases, the oscillating damped behavior of J_{ij} can be observed. We can see that for $D0_3$ structure, the strongest ferromagnetic interaction ($J_{ij} > 0$) is found between nearest-neighbors Fe_1-Fe_2 (which are located at 4*b* and 8*c* Wyckoff positions, respectively). In a case of $L1_2$ structure, the ferromagnetic contribution to the total exchange energy between nearest neighbors is found to be slightly smaller. Moreover, it is seen that in the second coordination shell ($d/a = 1$) for $L1_2$ structure, the Fe-Fe exchange parameters split into two FM contributions. In this case, each Fe at the distance of a_0 interacts ferromagnetically with six nearest neighbors: two Fe atoms provide $J_{ij} = 7.03$ (7.14) meV (GGA (LDA)) and four Fe atoms locating in (x, y) plane provide J_{ij} =2.59 (2.65) meV (GGA(LDA)), respectively. As can be seen, the difference between values J_{ij} obtained with two approximations is rather small, especially for $L1_2$ phase (see the inset in Fig. 3b).

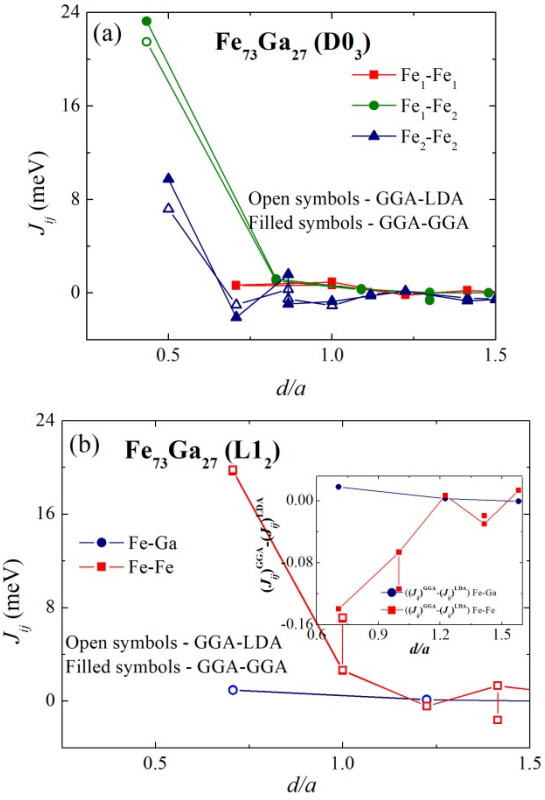

Fig. 3. The calculated exchange interaction parameters J_{ij} as a function of distance (d/a) between atoms i and j for the crystal structures (a) $D0_3$ and (b) $L1_2$ of $Fe_{73}Ga_{27}$ alloy. The inset shows the difference $\Delta J_{ij} = (J_{ij})^{GGA}$-$(J_{ij})^{LDA}$ between values of J_{ij} obtained with GGA and LDA approximations, respectively.

The knowledge of the constants of magnetic exchange interactions and magnetic moments allows us to simulate the temperature dependences of magnetization and to estimate the Curie temperatures for both investigation structures by means of Monte Carlo simulations of the classical Heisenberg Hamiltonian without a magnetic anisotropy term.

Fig. 4 shows the results of evaluations of the Curie temperature for the crystal structures of $D0_3$ and $L1_2$ of

$Fe_{100-x}Ga_x$ alloys. In general, theoretical results of Curie temperature estimations are in a good agreement with experimental data [4, 22]. It should be noted that the using of the magnetic exchange interactions obtained for GGA-LDA approach gives the results, which are the closer to the experimental data.

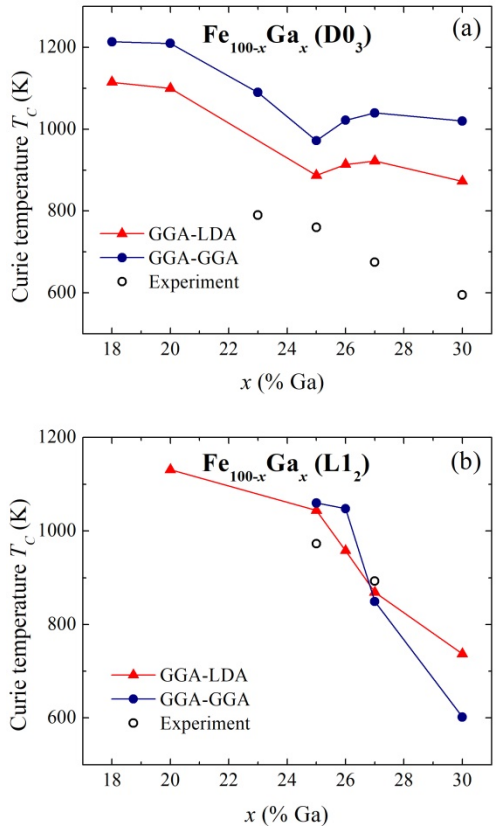

Fig. 4. The Curie temperature for the crystal structures (a) $D0_3$ and (b) $L1_2$ of $Fe_{100-x}Ga_x$ alloys in comparison with experimental data, which were taken from [4, 22].

4 Conclusion

In this work, we have introduced ab initio calculations and Monte Carlo simulations to study the structural and magnetic properties of $D0_3$ and $L1_2$ phases of $Fe_{100-x}Ga_x$ (x = 18 – 30%). The geometric optimization of $D0_3$ and $L1_2$ structures and calculations of exchange magnetic interactions have been performed by using the SPR-KKR package with treated of exchange-correlation energy in different approximations. It is shown that for the ground state calculations of both $D0_3$ and $L1_2$ structures of Fe-Ga alloys, the using of the GGA-PBE functional gives better results than LDA-VWN. However, The LDA-VWN approximation is favored for calculations of the exchange parameters J_{ij} and estimation of Curie temperatures by using the MC simulations of Heisenberg model. For the latter case, the theoretical values of Curie temperature of studied compositions for both phases are found in the better agreement with experimental ones.

Acknowledgments

This work is supported by Russian Science Foundation No. 17-72-20022 (LDA calculations) and No. 18-12-00283 (GGA calculations).

References

1. Q. Xing, Y. Du, R.J. McQueeney, T.A. Lograsso, Acta Mater, **56** 4536 (2008)
2. A.E. Clark, K.B. Hathaway, M. Wun-Fogle, J.B. Restorff, T.A. Lograsso et al., Jpn J Appl Phys, **93** 8621 (2003)
3. A.E Clark., M. Wun-Fogle, J.B. Restorff, T.A Lograsso., J.R. Cullen, IEEE Trans Magn, **37** 2678 (2001)
4. I.S. Golovin, A.M. Balagurov, I.A. Bobrikov, V.V. Palacheva, J. Cifre, J Alloy Compd, **675** 353 (2016)
5. T.A. Lograsso, A.R. Ross, D.L. Schlagel, A.E. Clark, J Alloys Compd, **350** 95 (2003)
6. I.S. Golovin, V.V. Palacheva, A.I. Bazlov, J. Cifre, J. Pons, J Alloy Compd, **644** 959 (2015)
7. I.S. Golovin, A.M. Balagurov, V.V. Palacheva, I.A. Bobrikov, V.B. Zlokazov, Mater. Des. **98** 113 (2016)
8. N. Kawamiya, K. Adashi, Y. Nakamura, J. Phys. Soc. Japan, **33** 1318 (1972)
9. R. Wu, Jpn J Appl Phys, **91** 7358 (2002)
10. T. Khmelevska, S. Khmelevskyi, P. Mohn, J. Appl. Phys. **103** 073911 (2008).
11. C. Paduani, C. Bormio-Nunes, J. Appl. Phys. **109** 033705 (2011)
12. H. Wang, Y.N. Zhang, T. Yang, Z.D. Zhang, L.Z. Sun, R.Q. Wu, Appl. Phys. Lett. **97** 262505 (2010).
13. H. Wang, Y.N. Zhang, R.Q. Wu, L.Z. Sun, D.S. Xu, Z.D. Zhang, Sci. Rep. **3** 3521 (2013)
14. Y. N. Zhang, R. Q. Wu, Phys. Rev. B **82** 224415 (2010).
15. Y. Zhang, R. Wu, IEEE Trans. Magn. **47** 4044 (2011)
16. Y. Zhang, H. Wang, R. Wu, Phys. Rev. B **86** 224410 (2012)
17. H. Ebert, D. Koedderitzsch, J. Minar, Rep. Prog. Phys., **74** 96501 (2011)
18. J. P. Perdew, K. Burke, M. Ernzerhof, Phys. Rev. Let., **77**, 18 3865 (1996)
19. S.H. Vosko, L.Wilk, M. Nusair, Canadian J. of Phys. **58** 1200 (1980)
20. A.I. Liechtenstein et al., J. Magn. Magn. Mater., **67** 65 (1987)
21. D.P. Landau, K. Binder, A. Guide to Monte Carlo Simulations in Statistical Physics, Cambridge, 2009
22. H. Okamoto, Bulletin of Alloy Phase Diagrams, **11** 576 (1990)
23. A.V. Ruban, I.A. Abrikosov, Rep. Prog. Phys. **71** 046501 (2008)